GOES I, J, K, L & M EPS

Dome Electron Channel

Calibration Report

February 16, 1988

Prepared for

Ford Aerospace Corporation
Western Development Laboratories Division
3939 Fabian Way
Palo Alto, California 94303-9981

by

PANAMETRICS, INC.
221 Crescent Street
Waltham, MA 02254

EPS Project Engineer	Paul B Morel	Date 2/16/88
Product Assurance	K. C. Smith	Date 2/16/88
Configuration Management	M. Quintal	Date 2/16/88
Program Physicist	Frederick A. Koons	Date 2/16/88
Program Manager	Bruce H Hilton	Date 2/16/88

TABLE OF CONTENTS

LIST OF ILLUSTRATIONS

LIST OF TABLES

1.0 INTRODUCTION

The EPS Dome Sensor for the GOES I-M spacecraft has been modified to incorporate three (3) electron channels in place of one on the earlier GOES spacecraft. The new design has approximate electron energy thresholds of 0.6, 2.0, and 4.0 MeV, with the channels designated E1, E2, and E3. The geometric factor for E1 and E2 (the single E1 of the earlier design) is also reduced to about 5/6 of that for the earlier design to lessen detector radiation damage.

The GOES D-H E1 (2.0 MeV threshold, = new E2) electron channel was calibrated with proton beams and beta sources, as reported in Ref. 1. The modified design for E1, E2, and E3 has been given a more extensive calibration with electron beams from the RADC Linear Accelerator, and with beta sources at Panametrics' facility. The Electron Calibration Plan is described in Ref. 2, and the calibration results are presented in this Calibration Report.

Section 2 contains a summary description of the Dome electron channels, with a short theoretical analysis of the expected responses. The electron calibration data taken at the Rome Air Development Center (RADC) Electron Linear Accelerator at Hanscom AFB, Massachusetts are described in Section 3, as are the beta source data taken at Panametrics' facility in Waltham, Massachusetts. The data analysis and results are presented in Section 4, and includes a comparison with the earlier calibration data and corrections to the D3 dome channel geometric factors because of the reduced FOV.

The new E2 geometric factor is 0.043 cm^2-sr for 2-3 MeV electrons, and is slightly larger than the 0.034 cm^2-sr for the old E1 in Ref. 1. The electron channel calibration in Ref. 1 used a beta source measurement to determine a 10% detection efficiency for electrons above 2 MeV, and applied this to the measured proton geometric factor of 0.34 cm^2-sr to obtain the total electron geometric factor. Correcting for the reduced FOV, the new electron calibration converts to 0.055 cm^2-sr for the old E1 (> 2 MeV) electron channel, which is about 60% larger than in Ref. 1. This is due to electron scattering increasing the off-normal-incidence detection area, and is discussed more fully in Section 4.5.

The summary and conclusions are contained in Section 5.

2. EPS DOME ELECTRON CHANNEL DESIGN

The EPS Dome Sensor for the GOES I-M spacecraft views the ambient particle fluxes through a multilayer insulation blanket. This blanket has an average thickness of 0.0264 g/cm^2 which is

primarily Kapton, Mylar, and Dacron (Ref. 3). Using the stopping power ratios of Al (Ref. 4) to Nylon and Mylar (Ref. 5) for 5-50 MeV protons, the thermal blanket is equivalent to about 1.30 times as much Al, or to 0.0343 g/cm^2 Al. For electrons in the range 0.2-2 MeV the stopping power ratio for lucite and Al in Ref. 6 average to 1.22, so this increased Al thickness is also appropriate for electrons.

The Dome detector cross section is shown in Fig. 2.1. The D3 moderator in the modified design is reduced to allow for the effects of the thermal blanket. As shown, the D3 FOV is also decreased slightly to reduce radiation damage effects on the solid state detectors, since the D3 detectors have the least amount of shielding for a large exposure solid angle. Except for these changes, the Dome design is identical to that of Ref. 1. The additional electron channels are added through changes in the electronics design, as discussed in the following sections.

2.1 D3 Dome and E1, E2 Electron Channels

The D3 dome has the new E1 channel with a threshold < 0.6 MeV, and the new E2 (old E1) channel with a threshold of 2.0 MeV. The particle energy loss curves for the D3 detectors (two 25 mm^2 area, 1500 micron thick surface barrier detectors) are shown in Fig. 2.2. The E1 channel has a threshold level logic of $6\cdot\overline{7}$, and a nominal electron energy threshold of 0.5 MeV based on range-energy calculations. The E2 channel has a threshold logic of $6\cdot7\cdot\overline{8}$, and has a nominal 2 MeV electron threshold.

The energy dependent geometric factor can be written approximately as

$$G(E) \sim 4\theta_1\, T(E)\, e(E')\, A_d\, (1-\cos^2\theta_2) \qquad (2.1)$$

where $\theta_1 \sim 31.9^\circ$ is the half angle to the front detector center in the $\pm 25^\circ$ direction of Fig. 2.1, $\theta_2 \sim 51.4^\circ$ is the same for the $\pm 45^\circ$ direction, $e(E')$ is the electron detection efficiency of the solid state detectors with the approximate threshold and particle energy E' incident on the detector, $A_d \sim 0.25$ cm^2 is the detector area, and

$$\begin{aligned} T(E) &\sim 1.5\,(1 - E_s/E), \quad E_s \le E \le 3\,E_s \\ &= 1 \qquad\quad , \quad E > 3\,E_s \\ &= 0 \qquad\quad , \quad E < E_s \end{aligned} \qquad (2.2)$$

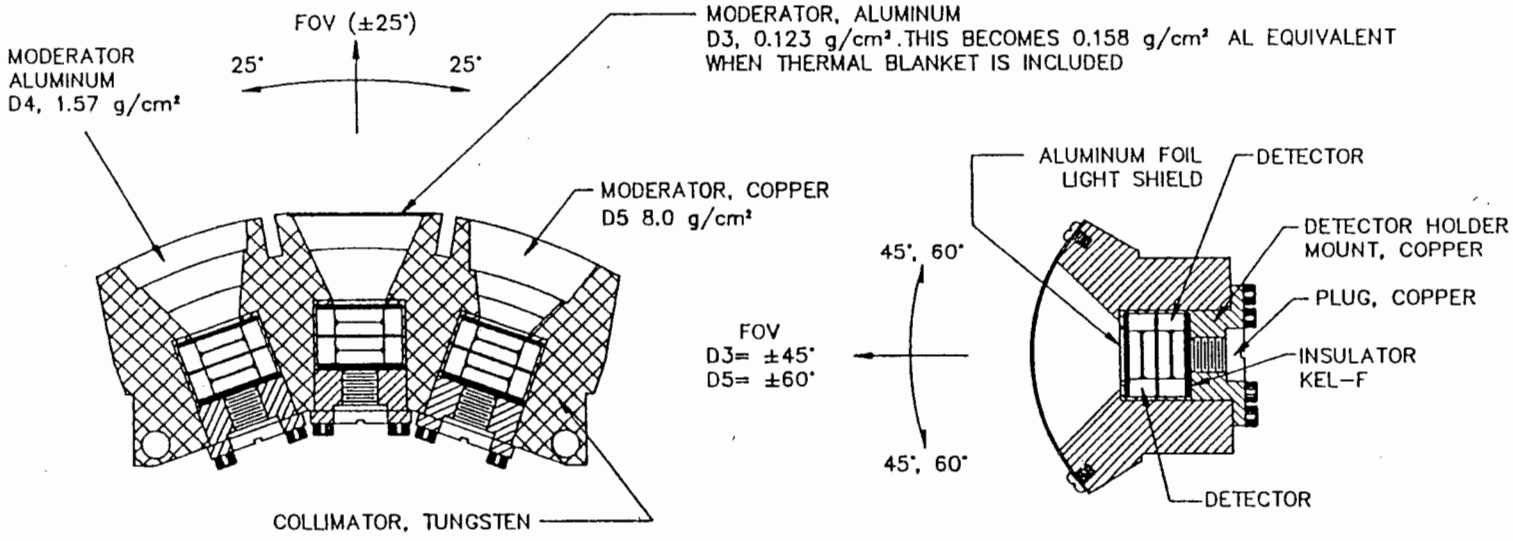

Fig. 2.1. Modified Dome Detector Cross Section.

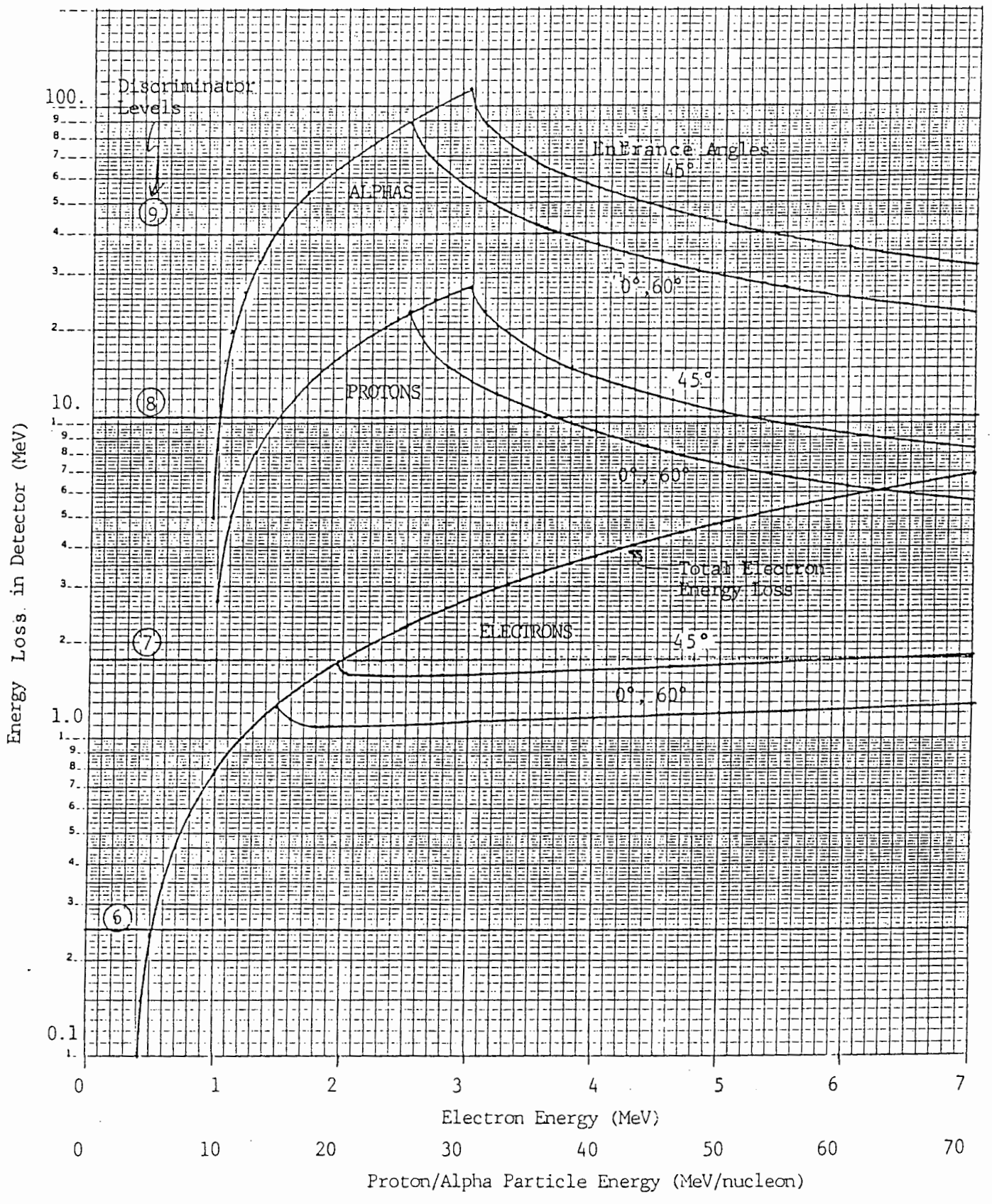

Fig 2.2. D3 ENERGY LOSS AND DISCRIMINATOR LEVELS DIAGRAM

is the approximate shield transmission fraction for electrons of incident energy E, with the shield thickness range energy being E_S.

The transmission function (2.2) is based on the measured detection efficiency rise of a detector under different thicknesses of Al hemispheres reported in Ref. 7, and is reasonably consistent with the electron transmission fractions shown in Ref. 8 (Fig. 1.2, p. 612) when the electron ranges of Ref. 6 are used. Note that the ranges in Ref. 6 are the average total pathlength for electrons, and are approximately equal to the linear material thickness that will just stop all (most) electrons from penetrating. The transmission factor (2.2) arises from the large amount of scattering which electrons undergo when losing energy in matter.

The characteristics of the E1 and E2 channels are summarized in Table 2.1, which includes theoretical G(E) calculations from (2.1). For E1 the e(E) values near threshold are estimates based on the approximate width of the residual energy distribution of the electrons after penetrating the (total) moderator thickness. The E2 value of e(E) = 0.1 for $E \geq 2$ MeV is based on the measured detection efficiency of Ref. 1. The calculation is approximate since it neglects the precise form of the shape at the extreme angles, using a sharp cut-off when approximately half the front detector area is covered, and it takes only approximate account of electron scattering affects. The actual calibrated geometric factors are given in Section 4.4.

2.2 D4 Dome and E3 Electron Channel

The D4 dome has the new E3 electron channel with a threshold $\geq$ 4.0 MeV. The particle energy loss curves are shown in Fig. 2.3, along with the threshold levels. The E3 threshold logic is 10·11, and the approximate geometric factor can be calculated from (2.1) with θ_2 - 62.2°. The D4 moderator has an electron range energy E_S = 2.55 MeV, and this is used in (2.2) to calculate the transmission fraction for higher energy electrons (below 3 E_S = 7.65 MeV). The detection efficiency $e(E_S)$ should be slightly higher than 0.1 for electrons above about 5 MeV. For electrons near 4 MeV the detection efficiency is calculated from the moderator transmitted electron energy spectrum, assuming a normal (Gaussian) distribution with a standard deviation of 0.25 times the energy loss in the moderator (s_E = 0.25 x 2.47 = 0.62 MeV). The fraction of electrons with energy above 1.53 MeV (the threshold) is multiplied by an assumed detection efficiency of 0.1 (high energy lower limit) to get the total $e(E_e)$.

The characteristics of the E3 electron channel, including the approximate calculated $G(E_S)$, are given in Table 2.2. The calculated geometric factor starts at about 3.5 MeV (10% of

Table 2.1

Characteristics of the D3 Dome E1 and E2 Electron Channels

D3 Dome moderator = 0.123 g/cm^2 Al

With thermal blanket, total = 0.158 g/cm^2 Al equivalent

Threshold levels: 6 = 0.25 MeV

7 = 1.77 MeV

8 = 10.5 MeV

Electron channel logic: E1 = $6 \cdot \overline{7}$

E2 = $6 \cdot 7 \cdot \overline{8}$

Approximate geometric factors from eq. (2.1):

E1				E2	
E_e(MeV)	$e(E_e)$	$T(E_e)$	G (cm^2-sr)	e ($E_e \geq 2$ MeV) - 0.1	
				e (MeV)	G(cm^2-sr)
0.39	0.00	0.00	0.00	$\geq$ 2	0.034
0.45	0.25	0.20	0.02		
0.50	0.50	0.33	0.06		
0.60	0.75	0.53	0.14		
0.80	1.00	0.77	0.26		
1.00	1.00	0.92	0.31		
$\geq$ 1.17	1.00	1.00	0.34		

Table 2.2

Characteristics of the D4 Dome E3 Electron Channel

D4 Dome moderator = 1.57 g/cm^2 Al (neglect thermal blanket effects)

Threshold levels: 10 = 1.53 MeV

11 = 5.6 MeV

Electron channel logic: E3 = $10 \cdot \overline{11}$

Approximate geometric factors from eq. (2.1) as modified for E3:

E_e(MeV)	$e(E_e)$	$T(E_e)$	G(cm^2-sr)
3.5	0.020	0.20	0.004
3.8	0.038	0.49	0.008
4.0	0.050	0.54	0.012
4.3	0.070	0.62	0.019
4.5	0.080	0.65	0.023
4.8	0.090	0.70	0.027
5.6	0.100	0.82	0.036
$\geq$ 7.7	0.100	1.00	0.044

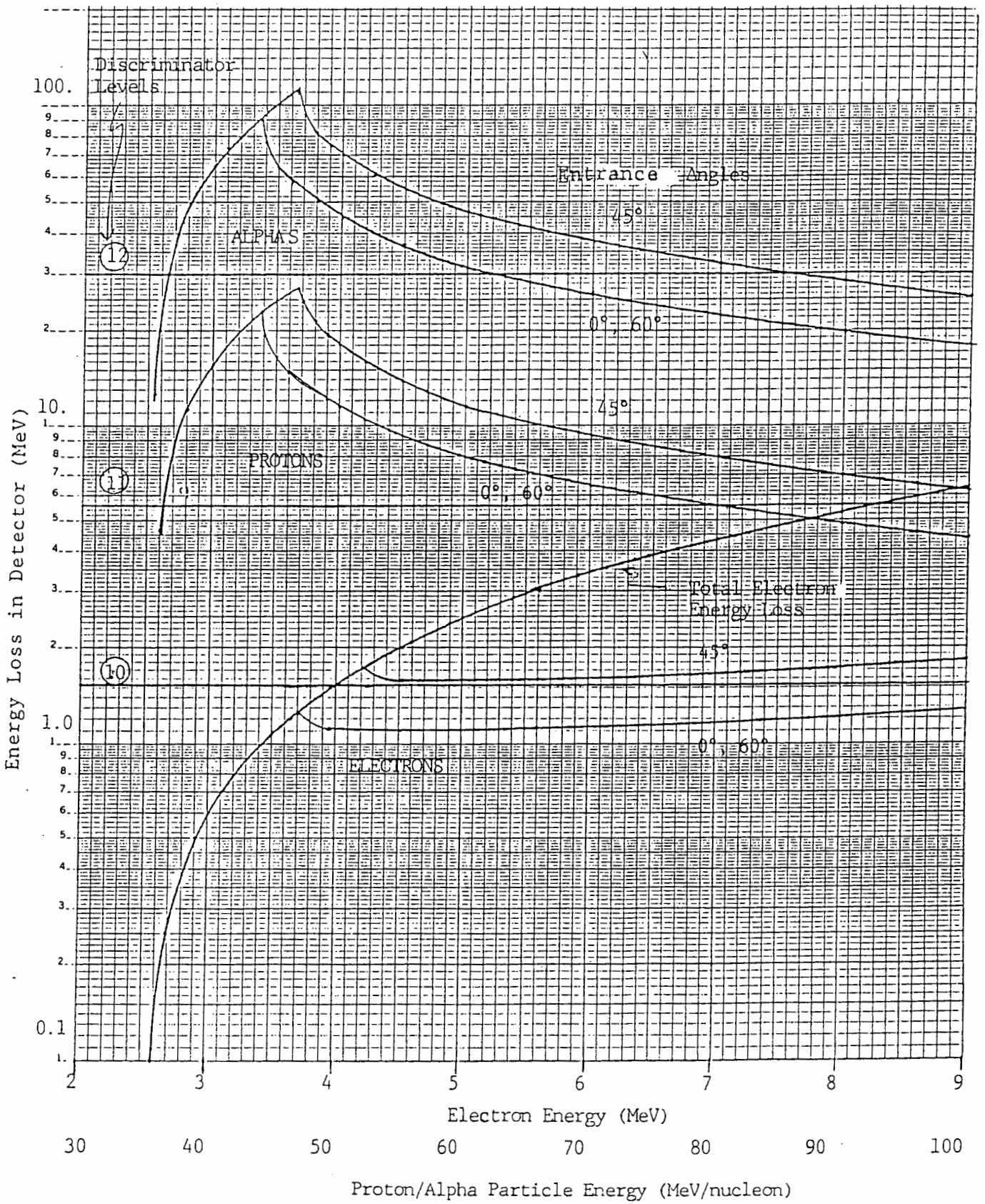

Fig. 2.3. D4 ENERGY LOSS AND DISCRIMINATOR LEVELS DIAGRAM

maximum), is half of maximum at 4.5 MeV, and is at the maximum of 0.044 cm^2-sr above 7.7 MeV. The energy dependent shape comes about equally from the electron transmission factor in (2.2), and the detection efficiency rise about 4.0 MeV. The actual calibration results for the E3 channel are given in Section 4.4.

3. EXPERIMENTAL CONFIGURATION AND DATA OBTAINED

3.1 Calibration at the RADC Linear Accelerator

The electron channel calibration at the RADC electron linear accelerator used the 30^o electron beam, with the Dome and monitor detectors configured as shown in Fig. 2.4. Two monitor detectors were used, a 750 micron, 2 cm^2 area detector (M1) with a 0.713 cm^2 area collimator, and a 1500 micron, 0.25 cm^2 area detector (M2) with a 0.173 cm^2 area collimator. The 1/2 inch Pb collimators have a range equivalent to 51.5 MeV electrons and are more than adequate for the 15 MeV maximum energy electron beam. The 750 micron M1 monitor detector is shielded from the rear by 1/4 inch Cu, which has a range equivalent to 9.3 MeV electrons, and so is well shielded from backscattered electrons. The two monitor detectors were used to verify a reasonably uniform intensity over the 8 inch wide calibration area. The higher counts from M1, as well as the better detector shielding, resulted in all Dome electron channel calibration data being normalized to the M1 counts for an area of 0.713 cm^2.

The electronics configuration is as shown in Fig. 2.5, which is as presented in Ref. 2. The MCA spectra were generally used to verify that the SCA settings were correct (below the minimum ionizing peak for the relativistic electrons), and that the detectors and electronics were operating properly. The primary data were the counts, and these were recorded in a Laboratory Notebook.

The RADC Electron Linear Accelerator can provide analyzed electron beams of 5 to 15 MeV at the 30^o bending port. Outside of this range the beam intensity is very low, and and data would be masked by background. The 5 MeV beam was degraded with Al absorbers to achieve three lower energies, although these become moderately broad in energy because of scattering in the absorbers. All electron beams are degraded by the accelerator exit window which consists of two Al windows with cooling water flow between them, and by the 50 inch air path. The total attenuation path is 0.20 g/cm^2 Al + 0.30 g/cm^2 H_2O + 0.15 g/cm^2 air, which is equivalent to 0.61 g/cm^2 H_2O, based on the relative stopping powers at 5 MeV in Ref. 6. The electron beam loses about 1.2 MeV in the external Al/H_2O/air path, and this produces about a 0.3 MeV standard deviation in the electron energy at the detectors (FWHM ~ 0.7 MeV). This becomes even larger for the three lowest energies, where additional Al absorbers are used. Data were taken without

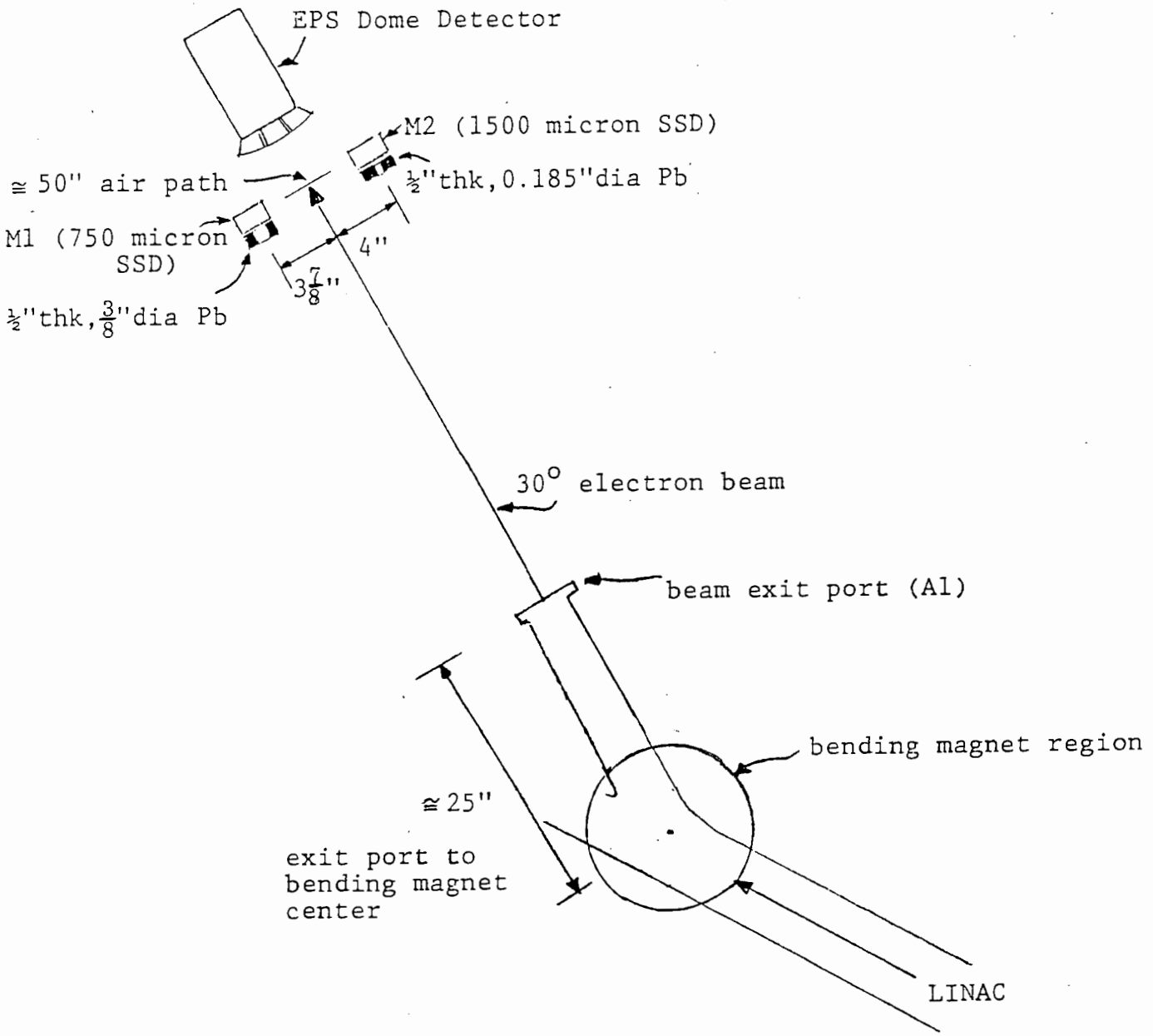

Fig. 2.4. Physical Configuration of Detectors and Accelerator at the RADC Electron Calibration.

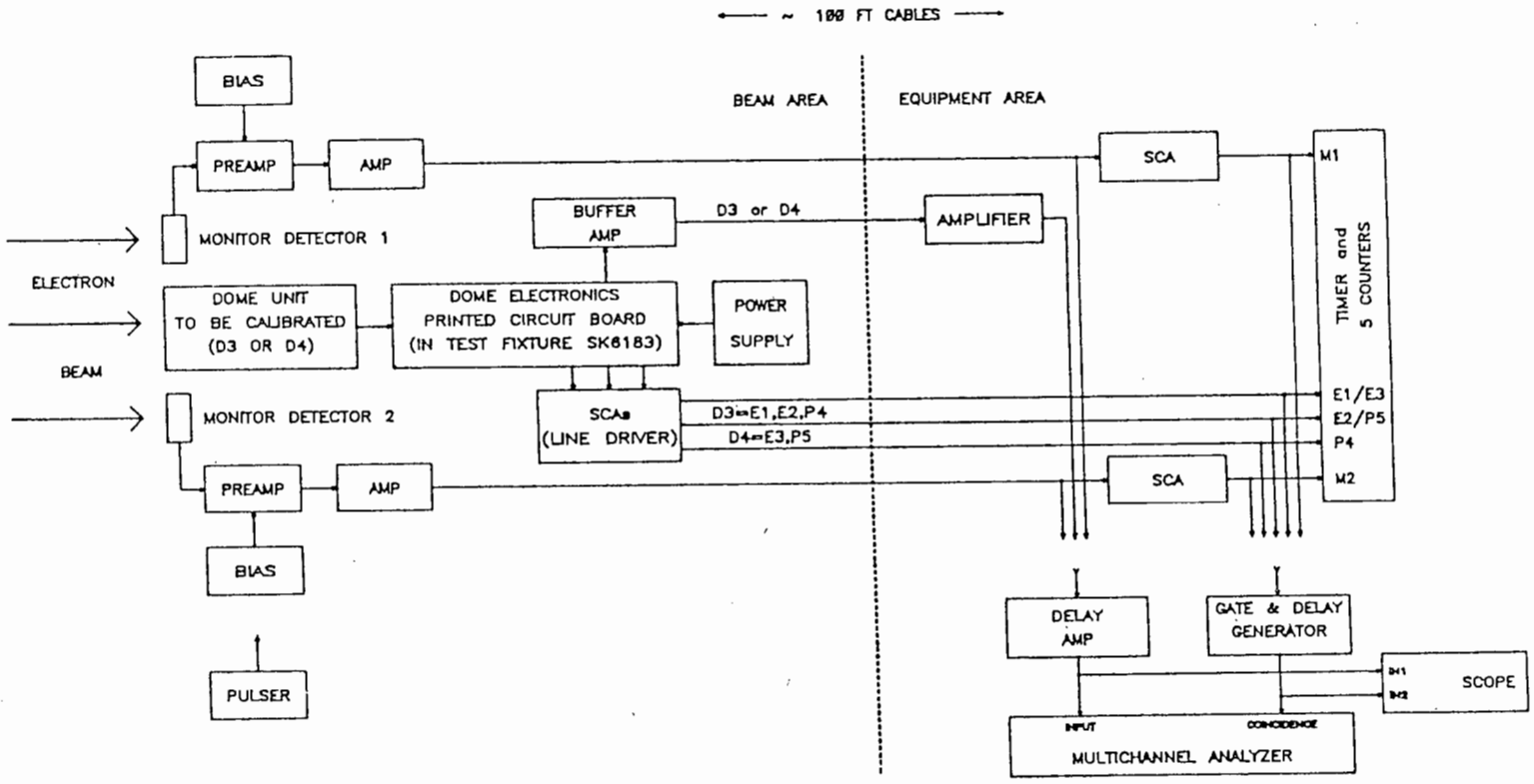

Figure 2.5. Electronics Test Configuration at the RADC Electron Linear Accelerator

Table 2.3

Electron Energies Used at RADC Accelerator Calibration

Initial Beam Energy (MeV) [1]	Absorbers Used (+ 0.61 g/cm^2 H_2O) (g/cm^2) [2]	Degraded Beam Energy (MeV) [3]	Approximate Standard Deviation (MeV) [4]
15	basic	13.6	0.3
10	basic	8.7	0.3
8	basic	6.8	0.3
6	basic	4.8	0.3
5	basic	3.8	0.3
5/4.1	+0.57 Al	2.9	0.5
5/2.9	+1.29 Al	1.8	0.8
5/2.2	+1.71 Al	1.1	1.0

[1]Electron beam energy selected by the magnet-energy in vacuum.

[2]Exit window + air path = 0.61 g/cm^2 H_2O equivalent is basic for all energies. Three lowest energies have additional Al absorbers added.

[3]Average electron energy incident on the Dome and monitors, before shield degradation, but corrected for the thermal blanket effects.

[4]Taken as 0.25 x (total energy loss in absorbers). This is likely to be an overestimate for the lowest energies, which are quite broad in energy spread.

the thermal blanket in front of the Dome sensor, but the incident electron energies were corrected for its effects. The correction is generally less than 0.1 MeV. The initial beam energies, the degraded beam energies (corrected for thermal blanket effects), and the estimated standard deviations, are in Table 2.3.

The Dome electron channels were calibrated at 0^{o}, 15^{o}, 30^{o}, 45^{o}, and 60^{o} (one energy only) in the θ_1 direction, i.e., along the $\pm$ 25^{o} angle range in Fig. 2.1. For the θ_2 direction data were taken at 0^{o}, 30^{o}, and 60^{o} (the $\pm$ 45^{o} (D3) and $\pm$ 60^{o} (D4) angle range in Fig. 2.1). Only one angle was varied so data had either $\theta_1 = 0^{o}$ or $\theta_2 = 0^{o}$. The angle scans were made at the eight energies listed in Table 2.3, except for the three lowest energies with the D4 (E3) channel. The angle scans obtained are listed in Table 2.4. These data were then analyzed and reduced to geometric factors as described in Section 4.

3.2 Calibration with Beta Sources

The D3 Dome with the E1 and E2 electron channels was also calibrated at Panametrics' Waltham facility with Sr-Y-90 and Ru-Rh-106 beta sources. The physical configuration for beta source calibration is shown in Fig. 2.6, while the electronics configuration was identical to Fig. 2.5 except for the 100 ft cables which were not needed. The total air path to the Dome detector was about 0.15 g/cm^2, and this is used to correct the beta spectra in the data analysis (Section 4.3).

The Sr-Y-90 beta source has 546 keV (maximum) electrons from Sr-90 and 2.27 MeV (maximum) electrons from Y-90. The air path and D3 absorber stop all electrons from Sr-90, so the source can be considered as only a Y-90 spectrum. For the Ru-Rh-106 beta source the Ru-106 has a 39 keV endpoint and Rh-106 a 3.54 MeV endpoint, so the source is effectively only Rh-106 for calibration.

The D3 (E1, E2) Dome was scanned through (θ_1, θ_2) angles of (0^{o}, 0^{o}), (15^{o}, 0^{o}), (30^{o}, 0^{o}), (45^{o}, 0^{o}), (0^{o}, 30^{o}), and (0^{o}, 60^{o}) for both beta sources. An additional measurement was made at (0^{o}, 0^{o}) with a sample of the thermal blanket material in front of the Dome detector to provide normalization to the configuration on the GOES I-M spacecraft. The beta source calibration data were analyzed as described in Section 4.3.

Table 2.4

Angle Scans Obtained for Electron Calibration at the RADC Accelerator

D3 Dome - E1 and E2 electron channels/P4 proton channel

Scans at (θ_1, θ_2) = (0°, 0°), (15°, 0°), (30°, 0°), (45°,0°), (0°, 30°), (0°, 60°)

Initial beam energies used (see Table 2.3) are:

15, 10, 8, 6, 5, 5/4.1, 5/2.9, and 5/2.2 MeV.

D4 Dome - E3 electron channel/P5 proton channel

Scans at (θ_1, θ_2) = (0°, 0°), (15°, 0°), (30°, 0°), (45°, 0°), (0°, 30°), (0°, 60°).

Initial beam energies used (see Table 2.3) are:

15, 10, 8, 6, and 5 MeV.

An additional point was measured at (60^{o}, 0^{o}) and 10 MeV.

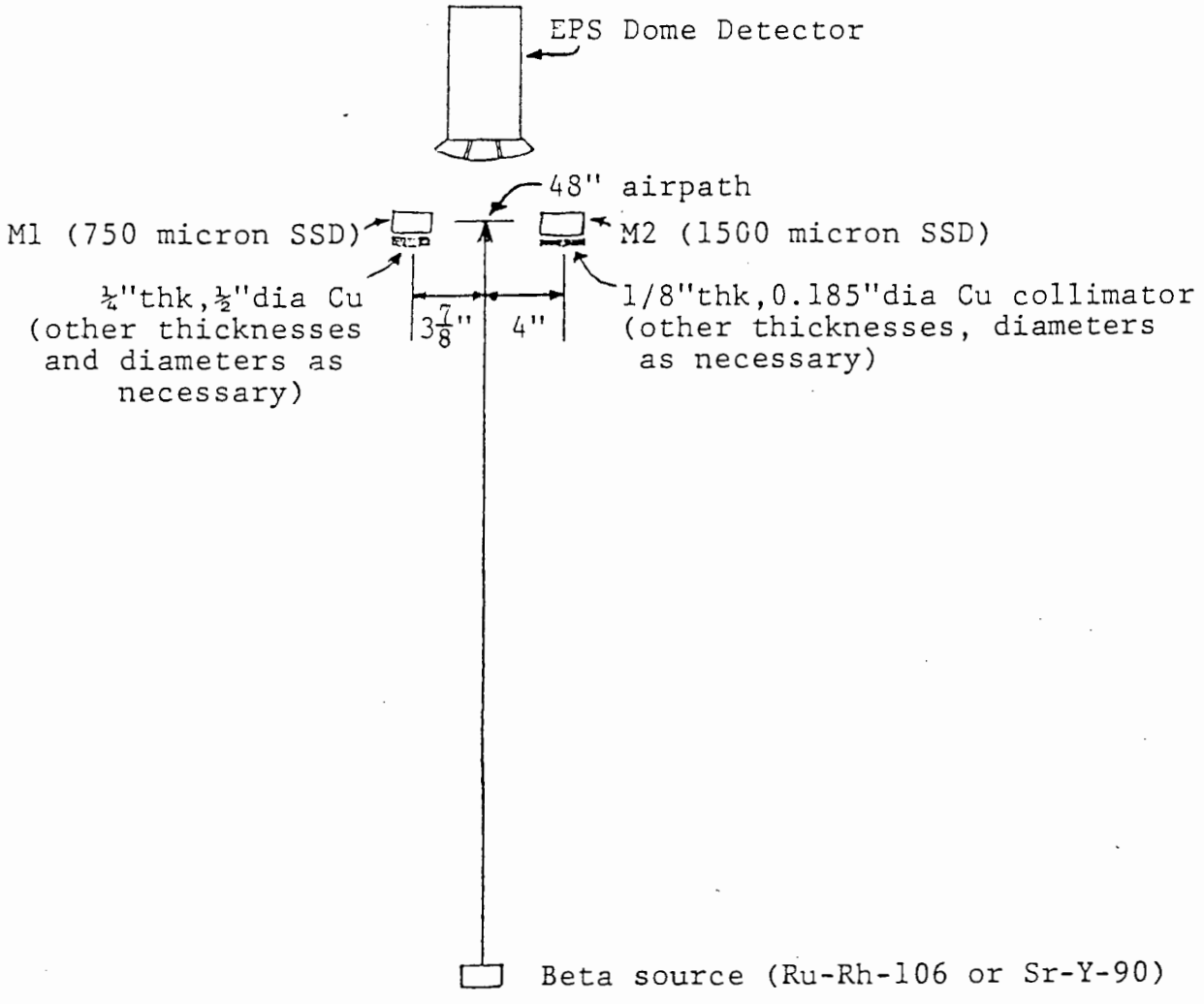

Fig. 2.6. Physical Configuration of Detectors and Beta Sources.

4. DATA ANALYSIS AND RESULTS

4.1 Geometric Factor Calculation

The geometric factors are calculated by using the measured areas, using the M1 detector count (0.713 cm^2 area) for normalization, and integrating over θ_1 and θ_2. Since scans are made only in θ_1 ($\theta_2 = 0$) and θ_2 ($\theta_1 = 0$), the values for other combinations are calculated by extrapolation using

$$A(\theta_1, \theta_2) = A(\theta_1, 0)\, A(0, \theta_2) / A(0, 0) \tag{4.1}$$

The shape of the D3 and D4 geometric factors is such that θ_1 corresponds to ϕ and $\theta_2 + 90^\circ$ to θ in the normal spherical coordinates (θ, ϕ) (note that this is the reverse of a complete (θ_1, θ_2) scan, as used in Ref. 1), so the total geometric factor is calculated from

$$G = \sum_{i,j} A(\theta_{1i}, \theta_{2j})\, D_{ij}\, n_{ij} \tag{4.2}$$

where D_{ij} is the solid angle increment

$$D_{ij} = \int_{D\theta_{1i}} d\theta_1 \int_{\theta_{2jl}+90^\circ}^{\theta_{2jh}+90^\circ} \sin\theta\, d\theta \tag{4.3}$$

$$= D\theta_{1i} (\sin\theta_{2jh} - \sin\theta_{2jl})$$

and n_{ij} are the number of equivalent bins of D_{ij} from symmetry. The values of D_{ij} and n_{ij} for the integrals are listed in Table 4.1.

The measured values of $A(\theta_1, \theta_2)$ (θ_1 or $\theta_2 = 0$) are calculated from the appropriate channel count and the simultaneously measured M1 count, both with background subtracted. Background is measured during periods when the beam is off, so it does not correct for beam-associated background, but the latter is

Table 4.1

Solid Angle and Bin Numbers For Geometric Factor Calculation

Value of (θ_1, θ_2) (deg)	Number of bins (n_{ij})	Range of angles θ_l, θ_h (deg) for θ_1	Range of angles θ_l, θ_h (deg) for θ_2	Solid angle increment, D_{ij} (sr)
(0, 0)	1	-7.5, 7.5	-15, 15	0.1355
(15, 0)	2	7.5, 22.5	-15, 15	0.1355
(30, 0)	2	22.5, 37.5	-15, 15	0.1355
(45, 0)	2	37.5, 52.5	-15, 15	0.1355
(0, 30)	2	-7.5, 7.5	15, 45	0.1174
(15,30)	4	7.5, 22.5	15, 45	0.1174
(30, 30)	4	22.5, 37.5	15, 45	0.1174
(45, 30)	4	37.5, 52.5	15, 45	0.1174
(0, 60)	2	-7.5, 7.5	45, 75	0.0678
(15, 60)	4	7.5, 22.5	45, 75	0.0678
(30, 60)	4	22.5, 37.5	45, 75	0.0678
(45, 60)	4	37.5, 52.5	45, 75	0.0678

not expected to be large. The pulse height spectra of the monitor detectors generally were well shaped Landau peaks from relativistic (minimum ionizing) electrons, and thus indicated that bremsstrahlung background was low. The geometric factors calculated from (4.2), based on the M1 monitor counts, were used as the calibrated electron geometric factors.

4.2 RADC Linear Accelerator Data Analysis

A typical set of calibration data taken at the RADC Linear Accelerator is shown in Table 4.2, which lists the measured areas for E1, E2, and E3 at an initial electron beam energy of 10 MeV, which corresponds to 8.7 MeV incident on the detectors (see Table 2.3). The areas are all normalized to the M1 monitor detector (0.713 cm^2), and statistical errors are on the order of 10% or less, except for the smallest values for each detector set. The (60^o, 0^o) data for E3 show a large drop from the (0^o, 0^o) and (45^o, 0^o) data, and indicate that the 45^o data limit in θ_1 is quite adequate. This factor was also used to eliminate taking any (0^o, 90^o) data, with the (0^o, 60^o) cut off being quite adequate.

The geometric factor calculation method is illustrated in Table 4.3, where the E1 geometric factor calculation from the 8.7 MeV electron data in Table 4.2 is shown. Using this method the resulting values for G are listed in Table 4.4, which also includes the A (0^o, 0^o) area values for reference. The listed electron energies are those for the sensor location, corrected for the effects of the thermal blanket. The thermal blanket was not used during the RADC accelerator calibration, and has an almost negligible effect on the electron energy at the high energies of the accelerator calibration. The results in Table 4.4 are compared with the theoretical calculations and are used to obtain a complete geometric factor vs. energy form in Section 4.4.

4.3 Beta Source Data Analysis

The Sr-Y-90 and Ru-Rh-106 beta sources provide continuous electron spectra to the end points of 2.27 MeV and 3.54 MeV, and this makes a geometric factor measurement more complex. The calibration is done by using the theoretical shapes vs. energy of Section 2, and normalizing the absolute geometric factor by use of the beta spectrum shape and measured source intensity. The beta spectra shapes are obtained from Ref. 9, and the source intensities were measured using the M1 monitor count rate and correcting for the measured fraction of the total beta spectrum which is detected. The beta spectra must be corrected for transmission through the 50 inch air path between the beta sources and the sensors.

Table 4.2

Calibrated Channel Detection Areas for 10/8.7 MeV Electrons

Angles (θ_1, θ_2) (deg.)	Measured area (cm^2) for E1	E2	E3
(0, 0)	0.731	0.045	0.043
(15, 0)	0.674	0.040	0.030
(30, 0)	0.356	0.016	0.024
(45, 0)	0.083	0.0032	0.0144
(60, 0)	---	---	0.0012
(0, 30)	0.626	0.037	0.039
(0, 60)	0.127	0.0045	0.0159

Areas are normalized to M1 monitor at 0.713 cm^2.

Accelerator-selected energy is 10 MeV; electron energy at sensor location is degraded to 8.7 MeV.

Table 4.3

Illustration of Geometric Factor Calculation Method

E1 calibrated area in (cm^2) for (θ_1, θ_2) at 10/8.7 MeV

θ_1 (deg) \ θ_2 (deg)	0	30	60
0	0.731	0.626	0.127
15	0.674	(0.577)	(0.117)
30	0.356	(0.305)	(0.062)
45	0.083	(0.071)	(0.014)

Numbers in parenthesis ( ) are extrapolated using eq. (4.1)

Total geometric factor calculated from eq. (4.2) using the values in Table 4.1 is

$$G = 1.065 \text{ cm}^2\text{-sr}$$

for an electron energy of 8.7 MeV at the sensor location.

Table 4.4

Geometric Factor and A (0^o, 0^o) Values from RADC Accelerator Electron Calibration

Electron Energy Incident on sensors (MeV)	Calibrated total geometric factor, G (cm^2-sr) for			Calibrated area at normal incidence, A(0^o,0^o) (cm^2) for		
	E1	E2	E3	E1	E2	E3
13.6	0.641	0.0244	0.0415	0.672	0.031	0.038
8.7	1.065	0.0559	0.0726	0.731	0.045	0.043
6.8	1.046	0.0453	0.0674	0.754	0.0385	0.0365
4.8	0.980	0.0565	0.0410	0.668	0.0441	0.0227
3.8	0.893	0.0558	0.0143	0.620	0.0433	0.0069
2.9	0.697	0.0436	--	0.526	0.0330	0.0070
1.8	0.576	0.0190	--	0.433	0.0153	--
1.1	0.487	0.0166	--	0.351	0.0099	--

The E1 and E2 channels of the D3 dome are the only ones that can be calibrated with beta sources. The D3 dome was irradiated using the geometry of Fig. 2.6, scanning the angles set listed in Section 3.2. The scans were made without the thermal blanket shield, and a normalization run was made at (0^o, 0^o) with a piece of thermal blanket in front of the Dome sensor. The angle scan data were integrated as described in Section 4.1 to give an effective geometric factor of

$$G = A_o\ (0^o,\ 0^o)\ D_o \tag{4.4}$$

The measured values of D_o for E1 and E2 for each beta source are listed in Table 4.5, and include all of the angular dependence of G, which is assumed not to vary with energy. The value of A_o (0^o,0^o) is set to the limiting (0^o,0^o) value for high energy electrons.

The value of A_o (0^o,0^o) is calculated from the measured count rate at (0^o,0^o) with the thermal blanket in place, C_m (counts/sec), and the measured total source intensity at the sensor, J_B (electrons/(cm^2-sec)). The values of J_B for the two beta sources used for the October 1987 period of the data are listed in Table 4.6. A_o (0^o,0^o) is calculated from

$$A_o(0^o,0^o) = C_m/(F_B\ J_B) \tag{4.5}$$

where F_B is the fraction of the full beta spectrum which reaches the detector and triggers the threshold. F_B is calculated from

$$F_B = \int T(E)\ E(E_d)\ j_B\ (E)\ dE \tag{4.6}$$

where T(E) is the electron transmission factor of (2.2), using the full attenuation path (source window + air path + dome moderator), $E(E_d)$ is the detection efficiency of the solid state detector, and $j_B(E)$ is the spectral shape of the beta source from Ref. 9, normalized to 1. For the calibration data $E(E_d)$ is normalized to 1.00 at high energy, and is approximated by a turn-on width when the energy E_d passes through the detector threshold. The turn-on width was only used for the E1 channel, since it is quite small (~ 0.15 MeV FWHM) for the E2 channel. The calibrated G (eq. (4.4)) provides a value for $G(\bar{E})$, where $\bar{E}$ is average detected beta particle energy, and can be used with the theoretical shapes from Section 2 to provide more precise values for G(E) at lower energies.

The final calibrated geometric factors from the beta source measurements are summarized in Table 4.7. No data are shown for

Table 4.5

Measured Angular Part of E1 and E2 Geometric Factors for Beta Sources

Beta Source type	End-point energy (MeV)	Measured values of D_o (sr) for electron channels E1	E2
Sr-Y-90	2.27	1.991	0.777
Ru-Rh-106	3.54	1.868	1.485

Table 4.6

Measured Beta Source Intensities at D3 Dome Sensor

Beta Source Type	Panametrics Source ID	Beta Spectrum Contribution	Total Electron Flux J_B (el/(cm^2-sec)) at 50 inches *
Sr-Y-90	#84	Y-90 only	1.263×10^3
Ru-Rh-106	#841	Rh-106 only	2.59×10^2

*Intensity is only for the one beta emitter listed, and for no air attenuation, i.e., in vacuum.

Table 4.7

Calibration Results From the Beta Source Data

D3 Dome Electron Channels

Electron Channel	Beta Source	Beta Spectrum	F_B value	C_m (cnts/sec)	G (max) (cm^2-sr)
E1	Sr-Y-90	Y-90	0.441	136.5	0.488
E1	Ru-Rh-106	Rh-106	0.667	51.2	0.554
E2	Ru-Rh-106	Rh-106	0.127	0.945	0.0460

E2 with Sr-Y-90 since the channel threshold of 2 MeV is too close to the beta spectrum end point of 2.27 MeV to give a statistically meaningful result. The data in Table 4.7 are combined with the RADC accelerator data to provide final overall calibration curves for the electron channels in the following Section 4.4.

4.4 Electron Channel Geometric Factors

4.4.1 E1 Channel

The beta source and accelerator calibration data are in excellent agreement. The Sr-Y-90 data with an average electron energy at the sensor of 0.93 MeV give G_{max} = 0.488 cm^2-sr, while the Ru-Rh-106 data with an average energy of 1.35 MeV give G_{max} = 0.554 MeV. The accelerator data give 0.487 cm^2-sr at 1.1 MeV and 0.576 cm^2-sr at 1.8 MeV. The accelerator data in Table 4.4 show a continuous slow rise with energy, to 1.065 cm^2-sr at 8.7 MeV. This rise is most likely due to the greater penetration of the higher energy electrons, which can undergo more scattering in the W collimator and still have enough energy to be detected when reaching a detector. The latter is reflected in the A (0^o, 0^o) areas of Table 4.4, which show a continuous rise with energy.

The 13.6 MeV G is lower than at 8.7 MeV, although the A(0^o,0^o) value does not drop very much. This is most likely due to less scattering in the D3 moderator which decreases the off-angle part of the geometric factor, as measured. From a practical point of view, the geometric factor drop at 13.6 MeV is not important because the overwhelming part of the E1 count rate comes from electrons in the 0.5 - 2 MeV range.

The theoretical shape of the initial rise of the E1 geometric factor in Table 2.1 can be normalized to 0.526 cm^2-sr, the average of the beta source (0.93 and 1.35 MeV) and low energy accelerator (1.1 and 1.8 MeV) calibration points, and combined with the higher energy accelerator calibration points, to yield the final E1 channel electron calibration data in Table 4.8. These data are also plotted in Fig. 4.1, along with the E2 and E3 final calibration data. The final electron calibration data are felt to be accurate to about $\pm$ 20%, and the shape of G(E) can be used to calculate absolute electron fluxes for a known j(E) spectral shape. Use of E1, E2, and E3 can allow the derivation of three independent parameters to describe the electron spectrum.

4.4.2 E2 Channel

The Ru-Rh-106 beta source calibration give 0.0417 cm^2-sr for an average energy above the detector threshold of 2.4 MeV. This is in good agreement with the 2.9 MeV accelerator data which give G = 0.0436 cm^2-sr, and the two average to 0.0427 cm^2-sr. The E2

Table 4.8

Final Calibrated Geometric Factors of the E1 Channel For Electrons

Electron Energy E (MeV)	Calibrated Geometric Factor G(E) (cm^2-sr)
0.39	0.00
0.45	0.03
0.50	0.09
0.60	0.21
0.80	0.41
1.00	0.48
1.17	0.53
1.8	0.58
2.9	0.70
3.8	0.89
4.8	0.98
6.8	1.05
8.7	1.07
13.6	0.64

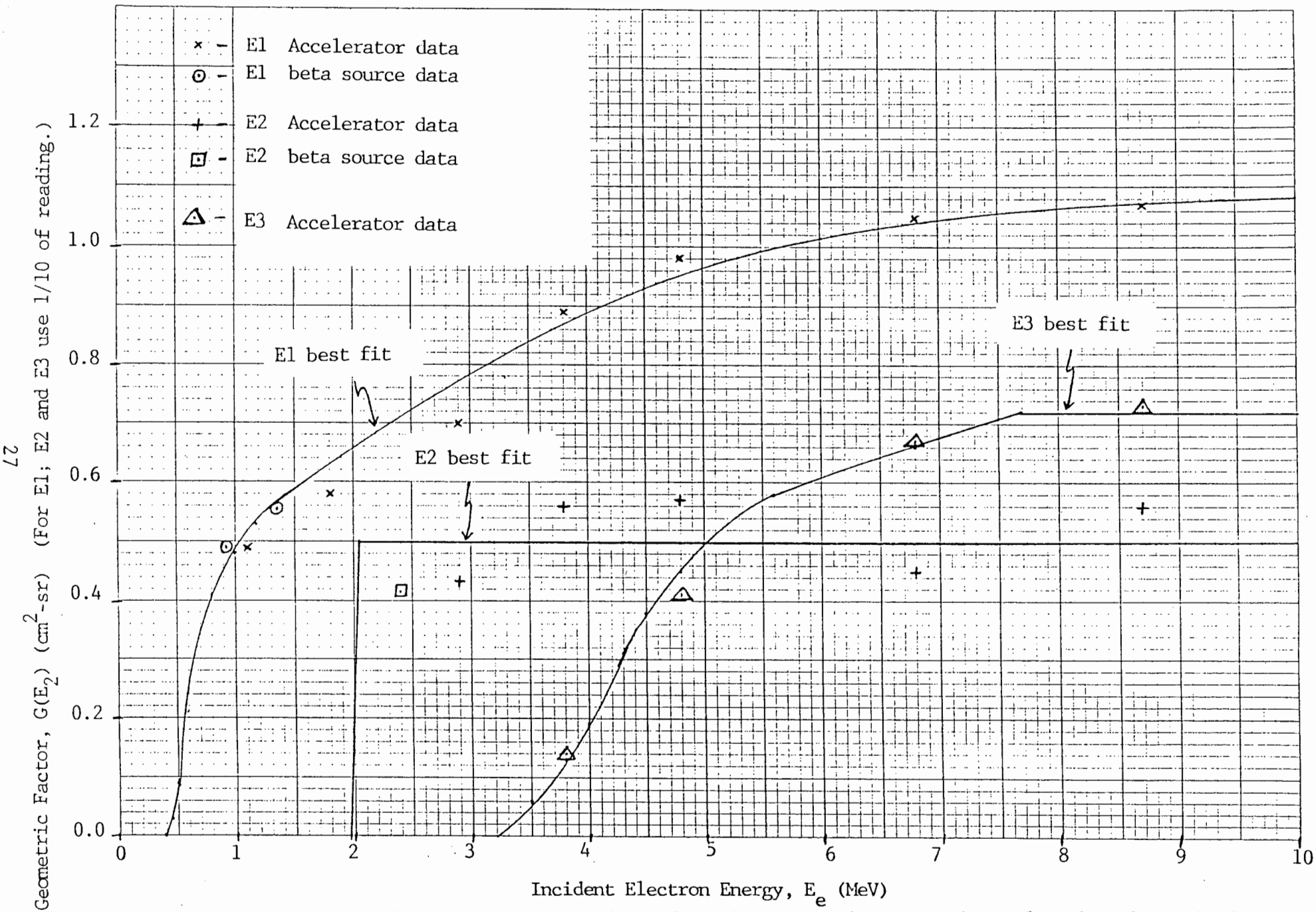

Fig. 4.1 Final Calibration G(E) Values for the Dome Electron Channels E1, E2, and E3.

channel has a sharp cut-on at 2 MeV, with a FWHM of about 0.15 MeV, which is negligible. The low energy part of G(E) can thus be taken as G(E) = 0.043 cm^2-sr for $2 \leq E < 3$ MeV, and the higher energy data taken from Table 4.4. The 1.8 MeV point in Table 4.4 results primarily from the energy spread of the incident electron beam (about 1.9 MeV FWHM), with the calculated fraction above 2 MeV giving about 0.0190 cm^2-sr, which is only 10% higher than the measured value. The 1.1 MeV value is also mostly due to beam energy width, which easily accounts for at least half the measured value. Uncertainty in the precise shape of the high energy tail of the 1.1 MeV beam, and the poor statistics (very low counts) in the E2 measurement indicate that the 1.1 MeV point can be discarded as a value for 1.1 MeV.

The final shape of G(E) for E2 is given in Table 4.9, and is plotted in Fig. 4.1. An average value of G(E) to about 10 MeV is 0.050 cm^2-sr, and this can be used as a good approximation for $E \geq 2$ MeV. For more precise work the shape in Table 4.9 can be used. The average value of 0.050 cm^2-sr when used with the Table 2.1 calculation data indicates that the detection efficiency for high energy electrons is about 0.147, while near threshold the 0.043 cm^2-sr measured G gives a detection efficiency of about 0.127. The estimated accuracy of G(E) is about $\pm$ 20%. The drop at 13.6 MeV is not completely understood, as it is a factor of about 2 in G and 1.5 in A (0^o, 0^o) (see Table 4.4). This may be an artifact of the upper limit energy of the RADC linear accelerator. It is not expected to be important since the dominant E2 channel count rate comes from electrons in the 2 to 10 MeV range, actually mostly near 2 MeV.

4.4.3 E3 Channel

The E3 channel calibration data in Table 4.4 can be compared with the calculations in Table 2.2 to yield an average ratio

$$\text{(E3, calibrated G)/(E3, calculated G)} = 1.64 \qquad (4.7)$$

Using this ratio, the effective detection efficiency for high energy electrons, which was taken as 0.1 for Table 2.2, is about 0.164. The higher detection efficiency is consistent with the lower threshold of 1.53 MeV, vs. 1.77 MeV for E2. The ratio (4.7) can be used with the calculated G(E) values in Table 2.2 to give the calibrate shape for E3. These calibrated values are listed in Table 4.10, along with the calibration measurements. The 50% of maximum G occurs at about 4.4 MeV electron energy. The calibrated G(E) are plotted in Fig. 4.1, and are estimated to be accurate to $\pm$ 20%.

Table 4.9

Final Calibrated Geometric Factors of the E2 Channel For Electrons

Electron Energy E (MeV)	Calibrated Geometric Factor G(E) (cm^2-sr)
$\geq$ 2 to 3	0.043
3.8	0.056
4.8	0.057
6.8	0.045
8.7	0.056
13.6	0.024

Average geometric factor $\geq$ 2 MeV to 10 MeV = 0.050 cm^2-sr.

Table 4.10

Final Calibrated Geometric Factors of the E3 Channel For Electrons

Electron Energy E (MeV)	Calibrated Geometric Factor G(E) (cm^2-sr)*
3.5	0.006/ -
3.8	0.013/0.014
4.0	0.019/ -
4.3	0.031/ -
4.5	0.038/ -
4.8	0.045/0.041
5.6	0.058/ -
6.8	0.066/0.067
7.7	0.072/ -
8.7	0.072/0.073
13.6	0.072/0.042

*Values listed are (normalized calculation)/(calibration data).

4.5 Comparison with Previous Electron Channel Calibration

Except for the θ_2 angle range, the new D3 dome E2 ($\geq$ 2 MeV) electron channel is identical with the old GOES D-H E1 channel, which was calibrated with a beta source in Ref. 1. The Ref. 1 calibration was made at (0^o, 0^o) incidence with Sr-Y-90, and primarily Ru-Rh-106, beta sources. The measurements gave a detection efficiency of 0.10 for the 1.77 MeV threshold, and this was factored with the proton P4 channel corrected geometric factor of 0.34 cm^2-sr to get 0.034 cm^2-sr for the old E1 channel.

The GOES D-H D3 Dome had a collimator side opening of $\theta_1 = \pm 25^o$, $\theta_2 = \pm 60^o$, which is identical to the D4 Dome angle range. From eq. (2.1) the geometric factors can be given as

$$G(D3,\ \theta_2 = \pm 60^o) = 1.74\ A_d\ cm^2\text{-sr} \tag{4.8}$$

and

$$G(D3,\ \theta_2 = \pm 45^o) = 1.36\ A_d\ cm^2\text{-sr} \tag{4.9}$$

Using the measured geometric factor near threshold of 0.043 cm^2-sr, from Section 4.4.2, the value corrected to the old E1 solid angle is

$$\begin{aligned} G(\text{old E1}) &= 0.034 \times 1.74/1.36 \\ &= 0.055\ cm^2\text{-sr} \end{aligned} \tag{4.10}$$

which is about 60% larger than the Ref. 1 calibration. About 27% of the increase comes from the larger detection efficiency (0.127 in Section 4.4.1, vs. 0.10 in Ref. 1), and the remainder comes from the wider angular spread of the calibrated electron response measured for this report.

The present calibration data thus give a corrected value for the old GOES D-H E1 channel geometric factor for electrons of 0.055 cm^2-sr. Since this is based on angular scans of the channel response, rather than solely a (0^o, 0^o) measurement for electrons with the angular response shape for protons, this newer value is expected to be more accurate. The result is to reduce the > 2 MeV electron fluxes for the GOES D-H E1 channels by about 40%. It should be noted that this affects only the calculated fluxes, and not the detector count rates which are the data archived by NOAA.

4.6 Proton and Alpha Particle Responses of D3 and D4 Dome Channels

The proton response of E2 (old E1), P4, and P5 were measured and reported in Ref. 1. The P5 response for protons remains the same, but the direct E2 (old E1) and P4 responses must be decreased by a factor of 0.78, the fractional decrease calculated using eq. (2.1). The "spurious", out-of-aperture responses of E2 (old E1) and P4 increase slightly (about 5%), but this is a small correction to a complicated and somewhat uncertain geometrical factor. The spurious responses of Table 3.4 in Ref. 1 can thus be readily used for E2 (old E1) and P4. The A4 channel alpha particle response should be modified in the same manner, with only the direct G being multiplied by 0.78.

The new E1 channel proton response can be estimated from the old E1 calibration data, adjusted for the lower energy loss window. The 1.77 MeV level 7 for E2 cuts off most low energy protons from E1, except for some edge cutting protons which lose only a small amount of energy in the depleted part of the solid state detectors. This will give E1 an estimated $G \lesssim 0.1$ cm^2-sr for protons in the range 10-120 MeV. Above 120 MeV protons can penetrate the W shield, and the E1 channel will acquire an omni-directional response similar to the old E1 (new E2). The dE/dx values for the 1.77 MeV threshold correspond roughly to 380 MeV protons (0^o and 60^o incidence, see Fig. 2.2) and > 1000 MeV protons (45^o incidence). Edge cutting protons can be detected, however, so it is estimated that G ~ 0.1 cm^2-sr for about 120 to ~ 500 MeV. Above 500 MeV the geometric factor should rise substantially to about 1.5 cm^2-sr (within a factor of 2 or 3 - the experimental correction found in Ref. 1). Since the 0.25 MeV threshold 6 is below the minimum ionizing energy loss for protons (except for extreme edge cutters) the E1 channel should be sensitive to protons of all greater energies, with approximately the same geometric factor.

The new E3 channel response to protons should be similar to the old E1 (new E2), since the 1.55 MeV level 10 is near the E2 (old E1) threshold of 1.77 MeV. The higher level (cut-off) is 5.6 MeV for E3 vs. 10.5 MeV for E2 (old E1), so some adjustments are required. Referring to the energy loss curves in Fig. 2.3, the E3 channel response to protons is estimated as ~ 0.15 cm^2-sr for 36-80 MeV, ~ 0.45 cm^2-sr for 80-120 MeV, and ~ 1.5 cm^2-sr for > 120 MeV. There is possibly a slight decrease above 500 MeV where the 0^o and 60^o energy loss curve goes below level 10 (1.55 MeV), but this is within the uncertainty of the Ref. 1 "spurious" responses.

The P5 and A5 channels should have the same response as given in Ref. 1, since the D4 dome design has not changed. The estimated proton responses, both "direct" and "spurious", are listed in Table 4.11 for E1, E2, P4 for D3, and for E3 for D4. The corrected A4 channel response for alpha particles is also listed. The new E1 and E3 proton responses are less accurate than

Table 4.11

Estimated Geometric Factors of the Modified Channels for Protons and Alpha Particles

D3 Dome - decreased solid angle design

E1 proton response: G $\lesssim$ 0.1 cm^2-sr, 10-120 MeV

- 0.1 cm^2-sr, 120-500 MeV

- 1.5 cm^2-sr, > 500 MeV

E2 proton response: G ~ 0.36 cm^2-sr, 32 - ~ 500 MeV

plus "spurious" response of Table 3.4 in Ref. 1

P4 proton response: G ~ 0.16 cm^2-sr, 15-44 MeV

plus "spurious" response of Table 3.4 in Ref. 1

A4 alpha particle response: G ~ 0.16 cm^2-sr, 60-180 MeV

plus "spurious" response of Table 3.5 (Ref. 1) for alpha particles, and Table 3.6 (Ref. 1) for protons

D4 Dome - electron channel response to protons

E3 proton response: G ~ 0.15 cm^2-sr, 36-80 MeV

- 0.45 cm^2-sr, 80-120 MeV

- 1.5 cm^2-sr, > 120 MeV

the other channel responses since they are extrapolated estimates from calibrated data for other channels, as discussed above. Note that the detailed calibration curves of G(E) in Ref. 1 can be used directly if the old E1 (new E2) and P4 curves have the scale readings multiplied by 0.78.

5. SUMMARY AND CONCLUSIONS

The modified design of the EPS Dome Detector, using a smaller geometric factor for the D3 detector and adding two electron channels, has been calibrated with electron beams and beta sources for the electron response. The calibration data have been analyzed and reduced to response curves G(E) for the three electron channels E1, E2 and E3. The proton channels have negligible response to electrons. The new E2 channel is identical to the old (GOES D-H) E1 channel, and the more detailed new calibration data indicate that the old electron geometric factor is about 60% low. The accelerator calibrations are more precise than the beta source calibrations because of the narrower energy range of electrons available.

The modified D3 Dome channels have slightly lower geometric factors for P3 and A4. These modified geometric factors, as well as the proton responses for the new E1, E2 and E3 channels have been estimated. A final set of revised geometric factors for protons and alpha particles has been provided.

REFERENCES

1. GOES D, E, F Progress Report, Energetic Particle Sensor Dome Calibration Work, Report PANA-GOESP-CR3, Panametrics, Inc., Waltham, MA (August 26, 1980).

2. EPS DOME Subassembly Electron Calibration Plan, NXT-TP-104, Rev. -, Panametrics, Inc., Waltham, MA (August 26, 1987).

3. FACC Memo, TC-86-179, GOES-PCC-TM-0690, J.C. Yee to G. Zwirn (17 November 1986).

4. J.F. Janni, Calculations of Energy Loss, Range, Pathlength, Straggling, Multiple Scattering, and the Probability of Inelastic Nuclear Collisions for 0.1 to 1,000 - MeV Protons. AFWL-TR-65-150 (1966).

5. J.F. Janni, Proton Range-Energy Tables, 1 keV - 10 GeV, Part 1, Compounds, At. Data and Nucl. Data Tables 27, No. 2/3, 148-339 (March/May 1982).

6. M.J. Berger and S.M. Seltzer, Tables of Energy Loss and Ranges of Electrons and Positrons, NASA SP-3012 (1964).

7. M.S. Gussenhoven, R.C. Filz, K.A. Lynch, E.G. Mullen, and F.A. Hanser, Space Radiation Dosimeter SSJ* for the Block 5D/Flight 7 DMSP Satellite: Calibration and Data Presentation, AFGL-TR-86-0065, Air Force Geophysics Laboratory, Hanscom AFB, MA (20 March 1986).

8. R.D. Evans, The Atomic Nucleus, McGraw-Hill, New York (1955).

9. O.H. Hogan, P.E. Zigman, and J.L. Mackin, Beta Spectra II. Spectra of Individual Negatron Emitters, USNRDL-TR-802 (16 December 1964).